HHS Public Access

Author manuscript

IEEE J Sel Top Quantum Electron. Author manuscript; available in PMC 2022 September 01.

Published in final edited form as:

IEEE J Sel Top Quantum Electron. 2021 ; 27(5): . doi:10.1109/jstqe.2021.3061462.

Plasmonic Gold Nanostar-Mediated Photothermal Immunotherapy

Ren A. Odion,
Biomedical Engineering Department, Duke University, Durham, NC 27708 USA

Yang Liu,
Chemistry Department and the Biomedical Engineering Department, Duke University, Durham, NC 27708 USA

Tuan Vo-Dinh [director]
Biomedical Engineering and Chemistry Department, Duke University, Durham, NC 27708 USA.; Fitzpatrick Institute for Photonics at Duke University.

Abstract

Cancer is among the leading cause of death around the world, causing close to 10 million deaths each year. Significant efforts have been devoted to developing novel technologies that can detect and treat cancer early and effectively to reduce cancer recurrences, treatment costs, and mortality. Gold nanoparticles (GNP) have been given particular attention for its use with photo-induced hyperthermia coupled with novel immunotherapy methods to provide a new platform for highly selective and less invasive cancer treatment. Among the various GNP platforms, gold nanostars (GNS) have a unique star-shaped geometric structure that allows superior light absorption and photothermal heating. This photothermal effect have also been found to amplify the anti-tumor immune response and can be exploited with adjuvant treatments using immune checkpoint inhibitors. This combination treatment known as Synergistic Immuno Photo Nanotherapy (SYMPHONY) has been shown to reverse tumor-mediated immunosuppression and has led to effective and long-lasting immunity against not only primary tumors but also cancer metastasis. This overview highlights the development and applications of GNS-mediated therapy developed in our laboratory for cancer treatment. This paper also presents recent results of experimental studies to illustrate the superior performance of GNS for photothermal treatment applications.

Keywords

Immunotherapy; immune checkpoint; hyperthermia; plasmonics; nanoparticle; nanostar; photothermal therapy; surface-enhanced Raman scattering (SERS); cancer

I. Introduction

Recently, gold nanoparticles have seen widespread usage as platforms for imaging, diagnosing, and treating cancer. They have been widely studied due to gold being relatively

corresponding author phone: 919-613-9145; tuan.vodinh@duke.edu.

inert in the body and their flexibility in size allows for selective distribution around the leaky vasculature of tumor sites [1]. Additionally, their gold surface allows for flexible chemical conjugation of dyes unto these particles making them excellent platforms for tumor imaging and detection. Furthermore, their most important property for therapy is their ability to convert photons to heat at a very high efficiency. Upon excitation with laser light, these nanoparticles act as a conduit for producing heat that can effectively heat and ablate tumor as needed. This unique feature is due to the effective plasmonic effect well known in GNPs, which have been used to great effect for photothermal conversion as well as other use cases in diagnostics utilizing optical phenomena such as Surface Enhanced Raman Scattering (SERS) [2]–[4]. Their facile synthesis, surface modifiability, tunable size, shape, optical properties, and biocompatibility have thus brought GNPs to the forefront in cancer research [2], [5], [6]. Photo-induced hyperthermia and ablation has long been used as a standard treatment of tumors by direct laser light contact, typically delivered via optical fibers [7]–[12]. Hyperthermia (HT) is a specific treatment wherein heat is applied to a tumor until temperatures of over 55 °C is reached, inducing immediate cell death at the target site [7], [8], [10]. These methods, however, have distinct disadvantages in that they require high amounts of laser power and are not spatially precise [13]. Commercial medical laser equipment used for tumor ablation can reach up to 10 W at 100% profile power for 2-second pulses with a 6-mm laser aperture [14]. Gold nanoparticle-mediated therapy provides an improved photon and heat delivery platform that promises to effectively treat tumors specifically, noninvasively, and at lower power requirements such as using less than 1 W/cm^2 [13]. This is important as it allows for more selected, targeted, and controlled heating at the target site for inducing cell death, rather than ablating large amounts of target and non-target surrounding tissue. Ideally the laser power should be at or lower than 0.2 W/cm^2, which is below the maximal permissible exposure of skin per ANSI regulation. In addition, the use of GNP offers the advantage of multiple treatment and imaging modalities to be used in conjunction with photothermal therapy (PTT) [15], [16]. For instance, additional uses include radio-sensitization of hypoxic regions, enhancement of drug delivery, activation of thermosensitive agents, and boosting the immune system [17]–[21]. In this paper we provide an overview of the GNS and its use in photothermal and immunotherapy of cancer *in-vivo*. Furthermore, we present the latest results of *in vitro* studies in solutions and gel phantoms to investigate the photothermal properties of GNS *in-vitro* to investigate the superior performance of GNS in light absorption and heat generation using different laser setups.

II. Nanoparticle Properties

A. Plasmonics and Gold Nanostars

Various nanoplatforms have been developed for photothermal therapy including gold nanospheres, gold nanoshells, gold nanorods, and gold nanostars [13], [22]–[28]. Among the different nanoparticles used for light induced PTT, gold nanostars (GNS) offer a particular advantage due to its unique star-shaped geometry and optical tunability [2], [5], [29]. Fig. 1 (a) depicts a contour plot of the magnitude of the electric field, which shows that the largest E-field enhancement that occurs at the tips of the branches of the star [3]. The large field enhancement at the tips of the star is due to a combination of the resonance enhancement and the lightning-rod effect associated with the large curvature at the tips. This curvature

creates a larger surface charge density and, consequently, a higher electric field. As a result, the nanostar can generate E-field hot spots that can greatly exceed the enhancement of smoother particles such as nanospheres. Fig. 1 (b) and (c) shows the transmission electron microscopy (TEM) image of the GNS along with a three-dimensional (3D) model of the EM field around the whole nanostar. The multiple sharp branches act as a “lightning rod” that enhances the local (EM) field dramatically resulting in the strong SERS effect in medical diagnostics and the effective heating seen in PTT for killing tumor cells in cancer therapy [2], [16], [19], [29]. Our team has devoted research efforts on the engineering and tuning of this tip-enhanced plasmonic property to target the ‘diagnostic-therapeutic’ optical window, a wavelength range in the near IR (700-1100 nm) wherein photons travel the farthest through tissue and thus have the most effective treatment range for the photothermal heating [5], [29]. More generally the optical windows can be divided in three groups NIR-I (700-1100 nm), NIR-II (1100-1350 nm), and NIR-III (1600-1870 nm) [30]. These optical windows represent other wavelength ranges that offer tradeoffs between less tissue scattering but more water absorption. Additionally, more specialized InGaAs camera detectors must be used for NIR-II and NIR-III spectral range; this requirement may limit more widespread applications than the usual silicon camera detectors used for UV to NIR-I spectral ranges. Since the peak plasmon absorption of GNS lies in the NIR-I region, the tissue optical window mostly involves the NIR-I range.

Gold nanostars are nanoparticles with several unique properties that make them highly effective for not only as photothermal agents but also as a contrast agent, immunotherapy adjuvants, and more [15], [16], [18], [29]. For example, we utilized the intrinsic TPL of GNS, acting as a contrast agent to track particles *in-vivo* to delineate vasculature and GNS, demonstrating the extravasation of nanostars [29]. In other applications, we demonstrated the synergistic effect of photothermal treatment with GNS coupled with an immunotherapy utilizing antibody immune checkpoint inhibitors [18]. Additionally, GNS may also be functionalized with other molecules to add functionality in fluorescence or Raman spectroscopy and imaging. Coupling a Raman-active dye on the surface of the GNS will produce a strong SERS signal that can be used for quantitative bio-sensing applications [3], [31]. Furthermore, the choice of Raman dye may also have a strong impact on the SERS signal as molecules whose absorption band coincides with the laser wavelength will exhibit a resonant SERS effect, often referred to as Surface-Enhanced Resonant Raman Scattering (SERRS). Conjugating other molecules such as the transactivating transcriptional activator (TAT) from human immunodeficiency virus 1 (HIV-1) can give the ability for the Raman-labeled GNS to penetrate the intracellular membrane of cells and be detected inside the nucleus [32]. These applications illustrate the versatility of the GNS platforms for a wide variety of use cases.

Numerous methods have previously been developed to generate the anisotropic features of the gold nanostars, utilizing surfactants such as Cetyltrimethylammonium Bromide (CTAB) or Polyvinylpyrrolidone (PVP) in order to facilitate its growth from colloidal gold particles [33], [34]. However, these surfactants are not biologically inert and thus prevents the gold nanostar’s wider use in biological experiments. To overcome these issues, our group has developed surfactant-free gold nanostars which are synthesized from 12 nm gold nanospheres that are reduced with gold chloride ($HAuCl_4$), silver nitrate ($AgNO_3$), and

ascorbic acid in a controlled manner under intense stirring [2], [29]. The GNS nanoparticles have multiple sharp branches that result in tip-enhanced plasmonics for imaging and PTT. The intrinsic absorption of the gold nanostar along with the source excitation play a crucial role in the conversion of light energy to heat. When a metallic nanostructured surface is irradiated by an EM field such as a laser, electrons in the conduction band are thrown into oscillations called surface plasmons. These oscillating electrons in turn produce a secondary electric field that adds to the incident field, thereby greatly increasing the conversion of photons to heat. This model was mainly derived from the Drude model of electrical conduction constrained at the nanometer scale of the particle [29]. The spectral absorption response of the respective nanoparticles across a large wavelength range were then simulated using analytical solutions with the simpler shapes such as the spheroid and finite element software (COMSOL Multiphysics) for the gold nanostar. The results of those theoretical studies show a the distinctly strong absorption for the GNS at the NIR wavelength range [35]. We have also investigated the electromagnetic field of various other plasmonic nanosystems such as nanospheres, nano-dimers, and nanoshells [22], [27], [28], [36], [37]. This EM field also gives rise to a very strong two-photon photoluminescence (TPL) from the resonant coupling of the GNS plasmon band and the incident laser [29]. The two-photon excitation is carried out by pulses of a femto-second laser, causing the simultaneous absorption of two photons on the GNS. The strong TPL effect is said to result from a recombination of electron-hole pairs as seen in other nanoparticles such as nanorods and produces among one of the highest two-photon action cross sections [29].

We have successfully demonstrated the effective us of GNS properties in imaging and therapy using glioblastoma (GBM) models in vivo [30]. Fig. 2 (a) and (b), which depicts the TPL image of the blood-brain barrier before and after photothermal treatment, effectively demonstrates the ability for selective, optically modulated delivery of nanoprobes into the tumor parenchyma with minimal off-target distribution by allowing the GNS to penetrate the blood-brain barrier (BBB) after thermal treatment [38]. The study illustrated the possibility for the use of GNS combined with a near IR laser to selectively open BBB for drug delivery into the brain for GBM treatment. We also performed electron microscopy to identify the subcellular location of the GNS in the brain tumor after intravenous injection through tail vein [39]. The brain tumor vasculature was found to be disrupted and became permeable for GNS. As shown in Fig. 2 (c), GNS were in both the tumor interstitial space and vasculature, suggesting GNS nanoparticles penetrate through the brain tumor vasculature via the enhanced permeation and retention (EPR) effect. Fig. 2 (d) shows that the GNS nanoparticles were localized in intracellular vesicles within the brain cancer cell. With 124I labeled GNS nanoparticles, we used PET/CT scan to measure brain tumor uptake of GNS to be about 7.2% ID/g [39].

Furthermore, we have extensively studied the multimodal functions of the GNS for combined capabilities for theranostics (i.e., therapy and diagnostics). This theranostics capability allows the GNS nanoprobe to be used for image-guided therapy for example. Fig. 2 (e) and (f) shows the different possible uses of the GNS diagnostic tool in imaging and spectroscopy [6], [16]. Fig. 2 (e) depicts the use of GNS labeled with positron emitter ^{64}Cu for PET imaging in 3D in vivo spatiotemporal tracking. In particular, the figure shows the selective accumulation of GNS around tumor periphery around after 24 hours. In Fig. 2 (f),

the Raman-active dye 4-Mercaptobenzoic (PMBA) are attached to the GNS to produce a strong and uniquely enhanced Raman spectral signal. This SERS effect is especially strong with GNS due to the tip-enhanced effect of the sharp branches of the nanoparticle. The figure shows the appearance of the unique SERS spectral peak at 1067 and 1588 cm-1 Raman shifts in the tumor site only, demonstrating the selectiveness of the GNS to accumulate in the tumor sites as confirmed with the other imaging modalities [16].

B. Synergistic Photothermal Immunotherapy

Immunotherapy has emerged as one of the most promising modalities to treat cancer. Immunotherapy with specific immune checkpoint inhibitor provides a promising way to break the tumor immunosuppressive environment [18], [20], [40]. Programmed death-ligand 1 (PD-L1), a protein overexpressed on cancer cell membrane, contributes to suppression of the immune system. PD-L1 binds to its receptor, PD-1, found on activated T cells, B cells, and myeloid cells, leading to modulation of T cell function [41]. The therapeutic anti-PD-L1 antibody is designed to block the PD-L1/PD-1 interaction and reverse tumor-mediated immunosuppression. Blocking the PD-L1/PD-1 axis has been shown to be highly beneficial in many human tumors and used as a cancer treatment modality [41]–[44]. However, current antibodies work only for a limited number of patients and can become ineffective with time. Generally, these anti-PD-L1/PD-1 antibodies play a role in inducing T cells to recognize tumors and allow for their destruction.

We have demonstrated that the combination of immune checkpoint inhibitor-based immunotherapy with GNS-mediated photothermal therapy has produced an effective two-pronged treatment modality referred to as Synergistic Immuno Photo Nanotherapy (SYMPHONY), which is designed to treat both primary and secondary tumor cell [18]. Fig. 3 (a) shows a schematic diagram of the operating principle of SYMPHONY using a dual flank tumor model in laboratory animal studies. First, localized PTT with GNS and NIR irradiation is used to kill primary tumor cells located in left flank of the mouse model (inset of Fig. 3 (a)). Upon GNS-PTT treatment, dying tumor cells after thermal ablation could release tumor associated antigens (TAAs), damage-associated molecular pattern molecules (DAMPs), heat shock proteins (HSPs), etc. when the cells are alive. DAMPs are intracellular molecules that are normally hidden. However, following cell damage or death DAMPS are released and acquire immunostimulatory properties. DAMPS exert various effects on antigen-presenting cells (APCs), such as maturation, activation and antigen processing/presentation [45]. APCs, which are present in the tissue or in local draining lymph nodes, process the tumor antigens and present tumor-derived peptides to T cells. Combining anti-PDL1 treatment with tumor antigen presentation will activate tumor-specific T cells that will attack both in the primary and distant/metastatic cancer cells. Therefore, following the combination treatment (PTT + anti-PDL1), the immune response can target the distant right flank tumor. This is particularly important in the primary tumor bed, hypoxic-oxygenated boundary, where it is believed metastatic/differentiating/proliferating potential is maximum. The Kaplan Meier curve in Fig. 3 (b) details the mouse survival of different treatment groups and shows the SYMPHONY group with a better outcome in survival. Additionally, a rechallenge was done on the SYMPHONY group after 150 days to show the treatment group's resilience from tumor recurrence. Fig. 3 (c) shows the mouse studies that revealed

that the two-pronged therapeutic approach, combining immune-checkpoint inhibition and GNS–mediated photothermal therapy, was effective in destroying primary treated tumors as well as untreated distant tumors in mice implanted with the MB49 bladder cancer cell line [18]. Specifically, distant tumor sizes did not increase in the SYMPHONY group. The effect of the combination of plasmonic GNS-enabled photothermal ablation and PD-L1 immunomodulation was demonstrated to be synergistic and not just additive. Furthermore, the delayed rechallenge with repeated MB49 tumor injections into cured mice did not lead to new tumor formation, indicating that the combined treatment induced effective long-lasting immunity, i.e., an anticancer ‘vaccine’ effect [18], [46].

C. Gold Nanostar-Mediated Photothermal Nanotherapy

As a principle, hyperthermia (HT), which is a treatment where heat is applied to a tumor or organ, aims to increase tumor temperature above physiologic body temperature with the goal of directly inducing cellular damage, as well as promoting local and systemic antitumor immune effects. Conventionally, hyperthermia is delivered using microwave, radiofrequency, high-intensity focused ultrasound, or heat applicators. However, these methods are not suitable for deep-seated tumors and the heating distribution is often not well controlled. Specifically, the optical penetration depth of a laser photon is inversely proportional to the square-root of the product of the absorption and scattering coefficients of the tissue [47]. This means that laser light is expected to decrease in energy before reaching deep-seated tumors farther away depending on the type of medium and tissue. It is noteworthy that Raman-labeled GNS could be detected in tissue phantom through the a monkey skull 5 mm thick, opening up the possibility for simultaneous heating and tumor detection [31]. These traditional methods are only macroscopically confined to the tumor area but cannot target or ablate cancer cells at the microprecision scale. Nanoparticle-mediated thermal therapy has recently received increasing interest [40], [48]–[54]. The ability to safely target single tumor cells with a high level of efficacy and specificity can be achieved with GNS. Their multiple sharp branches acting like “lightning rods” can convert safely and efficiently light into heat. We have performed a direct measurement of photothermal conversion efficiency for the 30 nm and 60 nm GNS, and we compared their efficiency to gold nanoshells, which are one of the most well-studied nanoparticles used for photothermal therapy. The results showed the temperature profiles for each of these three nanoparticles, with the 30 nm and 60 nm GNS having a much higher equilibrium temperature than nanoshells (34.7 °C) at equivalent optical density [49].

Rapid ablation can be achieved using GNS-mediated photothermal therapy by exploiting the natural propensity of nanoparticles to extravasate the tumor vascular network and accumulate in and around cancer cells. The significant reduction of the laser energy needed to precisely destroy the targeted cancer cells in which GNS preferentially accumulate due to the EPR effect [54], [55]. As shown before in Fig. 2, GNS selectively accumulate in tumors and we have even shown that we can use PTT to optically modulate delivery of nanostars into brain tumor in live murine models. Photothermal treatment on tumor vasculature may induce inflammasome activation, thus increasing the permeability of the blood brain-tumor barrier. Using GNS functionalized with cell penetrating peptides to facilitate the intracellular delivery followed by irradiation with a femto-second pulsed laser, a successful in vivo

photothermal therapy was achieved under an irradiance of 0.2 W/cm^2 [56]. These studies demonstrated that GNS have great potential for use in photothermal cancer therapy.

III. Investigations of photothermal effect of GNS

A. GNS Photothermal Heating

The choice in laser wavelength for excitation is also important because there is a marked difference in depth penetration as the laser source is further redshifted. Laser-based hyperthermia treatments are limited by the biological absorbers within tissue that effectively cut down the effective kill range possible. In the visible wavelength range (400-700 nm), hemoglobin is the primary absorber and may not be the intended target for a cancer therapy looking to ablate tumor masses that may be deeply embedded below the surface of the skin. In the NIR region (700-1100 nm), other chemical components such as melanin still play a major role in this absorption further blocking light. The ability for light to penetrate and heat tissue is thus a function of laser wavelength and the sum of the chemical absorbers in tissue.

One solution is the use of longer wavelength light to obtain better penetration depth through the skin. Most of the absorbing components in tissue typically decrease in absorptivity in longer wavelengths. By around 1100 nm, only water is a significant absorber in tissue. Another solution is to use fiberoptic delivery of laser directly to the tumor site through a small incision. Today, an emerging FDA-approved treatment for patients harboring intracranial tumors is laser interstitial thermal therapy (LITT), a minimally invasive technique that uses a stereotactically-guided laser at 1064 nm to ablate tumors. These devices are typically used to penetrate hard to reach targets like brain tumors. However, a major downside to their use is their non-specificity and high-power usage. Due to mentioned absorbers above, there is a potential for non-target heating and can possibly complicate the treatment. In addition, high powers are typically required to ablate tissue, leading to more uncontrolled heating or ablation of non-tumor tissue. GNS-mediated PTT attempts to solve this problem by reducing the need for high powered lasers and gaining more control in what is heated and for how long. The following studies evaluate the following options of laser wavelength and delivery method to evaluate an optimal configuration for GNS heating.

In this work, we investigated GNS-mediated PPT using the FDA-approved 1064-nm laser excitation. We evaluated the viability of 1064-nm excitation for PTT by quantifying the absorption coefficient of the GNS. This value is directly related to the absorption cross-section of the nanoparticle itself based on its shape as previously calculated theoretically and the concentration of GNS in the solution [35]. The absorption coefficient of GNS thus characterizes the heating characteristic of the GNS. Fig. 4 (a) shows the optical transmission configuration with a power sensor measuring the amount of light passing through a glass cuvette of GNS solution of different concentrations. Thermal measurements were collected for the duration of heating using thermocouples. The absorption of the GNS can then be calculated as a function of concentration using Beer’s law from a simple transmission setup. It is assumed that the attenuation of light is predominantly composed of the GNS absorption in the solution. A collimated beam delivered 0.3 W/cm2 power through the solution in the cuvette. The resulting collected data is displayed in Fig. 4 (b) which shows the exponential increases of GNS absorption at orders of magnitude dilutions near nanomolar concentration.

This result highlights the intense absorption of GNS at 1064-nm wavelength excitation. Furthermore, it underscores the fact that a very small amount of GNS (on the order of nanomolar concentration) was needed to absorb enough energy. As a point of comparison, the absorption coefficient of water at 1064 nm is about 0.144 cm-1 while that of GNS is 1.168 cm-1 at 0.1 nM concentration [57]. This stark difference in absorption indicated that there was much more selective and localized heating around GNS rather than the surrounding volume of water, showing the effectiveness of GNS-mediated PTT modality.

B. Quantitative Studies of GNS-Mediated Spatio-Temporal Heating

To quantify the photothermal characteristics of plasmonic nanoparticles, the well-known 2nd order differential heat flow equation was used to model the time evolution of heating of a volume of nanoparticles [58]. The source term was assumed to be a constant rate of heat production arising from a uniformly illuminated liquid volume of nanoparticles of specific concentration and specific absorption cross-section (calculated previously using the mentioned modified EM Drude models). The solutions to the heat equation yielded a dramatic increase in temperature within the first few minutes before slowly leveling off. Fig. 5 (a) shows the theoretical time-dependent heat equation solution for the GNS. In this study, this increase in heating was confirmed experimentally in Fig. 5 (b) which show the temperature of the solution starting at room temperature (21 °C) as a function of time by different concentrations of GNS. In particular, the rate of heating dramatically increases after 0.01 nM concentration while the water sample never increased more than a few degrees above ambient temperatures. It is noteworthy that the theoretical model reached higher temperatures as it assumed no heat perfusion, while the samples in the experiments have an air interface through which heat can be lost. To reach the temperatures obtained by GNS-mediated PTT, bare LITT (i.e., only laser without GNS) would require orders of magnitude higher power and possibly much longer treatment periods, all of which could lead to non-specific and off-target heating.

Since GNS preferentially accumulate due to the enhanced EPR effect, we also investigated the improved photothermal treatment efficiency of GNS-mediated PTT using tissue phantoms [16], [35]. In this study we investigated the improved effectiveness in heating GNS by using an experimental set-up like LITT that uses an optical fiber to deliver laser light directly into the target volume of a tissue phantom system. In previous photothermal mouse studies, we used inductively coupled plasma mass spectroscopy (ICP-MS) to determine that the concentration of GNS in tumors was approximately 0.1 nM. We used a lower concentration of GNS in our investigation of the heating change within the volume of GNS after laser irradiation. Fig. 6 (a) details the configuration where a gel phantom containing 0.04 nM concentration of GNS is heated using a fiber placed in the middle to deliver 808-nm laser light. The GNS-embedded gel phantom was used as the model system simulating a tumor that are infiltrated by GNS via the EPR effect. Three thermocouples at distances of 10 mm, 13 mm, and 15 mm were used to collect thermal data. Data collected using a thermal camera were also used to confirm the temperature measurements obtained with the thermocouples. The results in Fig. 6 (b) show a radially thermal heat map of the gel phantoms containing GNS (tumor model) and the gel phantom without GNS (normal tissue model). The heat map data clearly show the increase of heating radii in the GNS-containing

gel phantom compared to that without GNS at the same time point after 400 seconds. The result demonstrates that laser treatment delivered via an optical fiber can achieve superior effectiveness using GNS-mediated PTT.

IV. Conclusion

Gold nanostars fulfill an important need in expanding hyperthermia towards more effective and synergistic therapy modalities. Traditional hyperthermal therapies cannot target or ablate cancer cells at a precise enough scale and are thus bound to off-target heating and to its unintended effects. Nanoparticle-mediated PTT can selectively target tumor sites either by the EPR effect or through targeted binding towards specific cells. Photothermal treatment can be performed at much lower and safer laser powers as GNS more efficiently convert photons to heat than the surround water and tissue. Additionally, GNS with different sizes and branch numbers can be tuned to absorb laser energy at different wavelengths, allowing more flexibility towards additional modalities such as for imaging or spectroscopy. This multimodal functionality extends to additional therapeutic uses for the GNS as well, allowing them to act as trojan horses for drug delivery. Finally, GNS can be utilized for combined therapies, such as SYMPHONY, to leverage and enhance the effects of each individual therapies. Most promising is SYMPHONY acting as a cancer vaccine that not only eradicates primary ‘treated’ tumors but also results in the immune-mediated destruction of distant ‘untreated’ metastatic tumors.

The following could be further pursued to improve cancer imaging and treatment using GNS. In addition to passive targeting via the EPR effect, future studies can investigate active targeting using peptides or antibodies linked to GNS to improve tumor uptake. Of special interest is the synergistic combinatorial approach such as SYMPHONY that can reverse tumor-mediated immunosuppression, showing promise to treat not only unresectable primary tumors, but also distant cancer metastasis by enhancing the systemic activity of specific and adaptive immune responses and inducing an anticancer “vaccine” effect. Further studies will provide better understanding of the mechanisms underlying the novel synergistic treatment modalities of SYMPHONY to enhance and broaden the effect of immune-checkpoint inhibitors for successful eradication of metastatic cancer. Identifying, characterizing, and investigating the specific immune cells and molecular processes involved in this synergistic interaction will pave the way for successful treatment of locally advanced and metastatic cancer, and recurring tumors.

Acknowledgment

This work is supported by the National Institutes of Health, under award number 5R01EB028078-02.

Biography

Ren Odion received the B.Sc. degree in biomedical engineering from the University of California, Los Angeles in Los Angeles, CA, USA. He is currently working toward a Ph.D. degree in the Department of Biomedical Engineering at Duke University, Durham, NC, USA.

Yang Liu received the B.Sc. degree in analytical chemistry and M.S. degree in chemistry from Shanghai Jiao Tong University in Shanghai, China. He received his Ph.D. degree in chemistry from Duke University. He is currently a Postdoctoral Associate in the Department of Biomedical Engineering at Duke University, Durham, NC, USA.

Tuan Vo-Dinh received the Ph.D. degree in physical chemistry from ETH (Swiss Federal Institute of Technology) in Zurich, Switzerland, in 1975. He is currently the Director of the Fitzpatrick Institute for Photonics, R. Eugene and Susie E. Goodson Distinguished Professor of Biomedical Engineering, and a Professor of Chemistry at Duke University Durham, NC, USA. Prof. Vo-Dinh received seven RD-100 Awards for Most Technologically Significant Advance in Research and Development for his development of various technologies, the Gold Medal Award, Society for Applied Spectroscopy, the Languedoc-Roussillon Award, France, the Scientist-of the-Year Award, Oak Ridge National Laboratory, the Thomas Jefferson Award, Martin Marietta Corporation, and the Distinguished Inventors Award, Battelle Memorial Institute, the Exceptional Services Award for distinguished contribution to a Healthy Citizenry from U.S. Department of Energy, and the Award on Spectrochemical Analysis, American Chemical Society, and the Sir George Stokes Award, Royal Society of Chemistry.

References

[1]. Kalyane D, Raval N, Maheshwari R, Tambe V, Kalia K, and Tekade RK, “Employment of enhanced permeability and retention effect (EPR): Nanoparticle-based precision tools for targeting of therapeutic and diagnostic agent in cancer,” Materials Science and Engineering: C, vol. 98, pp. 1252–1276, 5 2019, doi: 10.1016/j.msec.2019.01.066. [PubMed: 30813007]

[2]. Khoury CG and Vo-Dinh T, “Gold nanostars for surface-enhanced Raman scattering: synthesis, characterization and optimization,” The Journal of Physical Chemistry C, vol. 112, no. 48, pp. 18849–18859, 2008.

[3]. Register JK et al., “In vivo detection of SERS-encoded plasmonic nanostars in human skin grafts and live animal models,” Anal Bioanal Chem, vol. 407, no. 27, pp. 8215–8224, 11. 2015, doi: 10.1007/s00216-015-8939-0. [PubMed: 26337748]

[4]. Harmsen S et al., “Surface-enhanced resonance Raman scattering nanostars for high-precision cancer imaging,” Science Translational Medicine, vol. 7, no. 271, pp. 271ra7–271ra7, 1. 2015, doi: 10.1126/scitranslmed.3010633.

[5]. De Silva Indrasekara AS, Johnson SF, Odion RA, and Vo-Dinh T, “Manipulation of the Geometry and Modulation of the Optical Response of Surfactant-Free Gold Nanostars: A Systematic Bottom-Up Synthesis,” ACS Omega, vol. 3, no. 2, pp. 2202–2210, 2. 2018, doi: 10.1021/acsomega.7b01700. [PubMed: 29503975]

[6]. Liu Y, Yuan H, Kersey FR, Register JK, Parrott MC, and Vo-Dinh T, “Plasmonic Gold Nanostars for Multi-Modality Sensing and Diagnostics,” Sensors, vol. 15, no. 2, Art. no. 2, 2. 2015, doi: 10.3390/s150203706.

[7]. Falk MH and Issels RD, “Hyperthermia in oncology,” Int J Hyperthermia, vol. 17, no. 1, pp. 1–18, 2. 2001, doi: 10.1080/02656730150201552. [PubMed: 11212876]

[8]. Hildebrandt B et al., “The cellular and molecular basis of hyperthermia,” Crit Rev Oncol Hematol, vol. 43, no. 1, pp. 33–56, 7. 2002, doi: 10.1016/s1040-8428(01)00179-2. [PubMed: 12098606]

[9]. Pandita TK, Pandita S, and Bhaumik SR, “Molecular Parameters of Hyperthermia for Radiosensitization,” CRE, vol. 19, no. 3, 2009, doi: 10.1615/CritRevEukarGeneExpr.v19.i3.50.

[10]. Wust P et al., “Hyperthermia in combined treatment of cancer,” The Lancet Oncology, vol. 3, no. 8, pp. 487–497, 8. 2002, doi: 10.1016/S1470-2045(02)00818-5. [PubMed: 12147435]

[11]. Schildkopf P et al., “Biological Rationales and Clinical Applications of Temperature Controlled Hyperthermia - Implications for Multimodal Cancer Treatments,” Current Medicinal Chemistry,

vol. 17, no. 27, pp. 3045–3057, 9. 2010, doi: 10.2174/092986710791959774. [PubMed: 20629627]

[12]. Frey B et al., "Old and new facts about hyperthermia-induced modulations of the immune system," International Journal of Hyperthermia, vol. 28, no. 6, pp. 528–542, 9. 2012, doi: 10.3109/02656736.2012.677933. [PubMed: 22690925]

[13]. Loo C et al., "Nanoshell-Enabled Photonics-Based Imaging and Therapy of Cancer," Technol Cancer Res Treat, vol. 3, no. 1, pp. 33–40, 2. 2004, doi: 10.1177/153303460400300104. [PubMed: 14750891]

[14]. Rennert RC et al., "Laser Ablation of Abnormal Neurological Tissue Using Robotic Neuroblate System (LAANTERN): Procedural Safety and Hospitalization," Neurosurgery, p. nyz141, 5 2019, doi: 10.1093/neuros/nyz141.

[15]. Liu Y et al., "Gold nanostar as theranostic probe for brain tumor sensitive PET-optical imaging and image-guided specific photothermal therapy," 2016.

[16]. Liu Y et al., "A plasmonic gold nanostar theranostic probe for in vivo tumor imaging and photothermal therapy," Theranostics, vol. 5, no. 9, p. 946, 2015. [PubMed: 26155311]

[17]. Brigger I, Dubernet C, and Couvreur P, "Nanoparticles in cancer therapy and diagnosis," Advanced Drug Delivery Reviews, vol. 64, pp. 24–36, 12. 2012, doi: 10.1016/j.addr.2012.09.006.

[18]. Liu Y et al., "Synergistic Immuno Photothermal Nanotherapy (SYMPHONY) for the Treatment of Unresectable and Metastatic Cancers," Scientific Reports, vol. 7, no. 1, 12. 2017, doi: 10.1038/s41598-017-09116-1.

[19]. Yuan H, Khoury CG, Wilson CM, Grant GA, Bennett AJ, and Vo-Dinh T, "In vivo particle tracking and photothermal ablation using plasmon-resonant gold nanostars," Nanomedicine: Nanotechnology, Biology and Medicine, vol. 8, no. 8, pp. 1355–1363, 11. 2012, doi: 10.1016/j.nano.2012.02.005.

[20]. Chen Q, Xu L, Liang C, Wang C, Peng R, and Liu Z, "Photothermal therapy with immune-adjuvant nanoparticles together with checkpoint blockade for effective cancer immunotherapy," Nature Communications, vol. 7, p. 13193, 10. 2016, doi: 10.1038/ncomms13193.

[21]. Wu G, Mikhailovsky A, Khant HA, Fu C, Chiu W, and Zasadzinski JA, "Remotely Triggered Liposome Release by Near-Infrared Light Absorption via Hollow Gold Nanoshells," J. Am. Chem. Soc, vol. 130, no. 26, pp. 8175–8177, 7. 2008, doi: 10.1021/ja802656d. [PubMed: 18543914]

[22]. Norton SJ and Vo-Dinh T, "Optical response of linear chains of metal nanospheres and nanospheroids," JOSA A, vol. 25, no. 11, pp. 2767–2775, 2008. [PubMed: 18978855]

[23]. Harris N, Ford MJ, and Cortie MB, "Optimization of Plasmonic Heating by Gold Nanospheres and Nanoshells," J. Phys. Chem. B, vol. 110, no. 22, pp. 10701–10707, 6. 2006, doi: 10.1021/jp0606208. [PubMed: 16771316]

[24]. Hirsch LR et al., "Nanoshell-mediated near-infrared thermal therapy of tumors under magnetic resonance guidance," PNAS, vol. 100, no. 23, pp. 13549–13554, 11. 2003, doi: 10.1073/pnas.2232479100. [PubMed: 14597719]

[25]. Link S and El-Sayed MA, "Spectral Properties and Relaxation Dynamics of Surface Plasmon Electronic Oscillations in Gold and Silver Nanodots and Nanorods," J. Phys. Chem. B, vol. 103, no. 40, pp. 8410–8426, 10. 1999, doi: 10.1021/jp9917648.

[26]. Yu Y-Y, Chang S-S, Lee C-L, and Wang CC, "Gold nanorods: electrochemical synthesis and optical properties," The Journal of Physical Chemistry B, vol. 101, no. 34, pp. 6661–6664, 1997.

[27]. Norton SJ and Dinh TV, "Spectral bounds on plasmon resonances for Ag and Au prolate and oblate nanospheroids," Journal of nanophotonics, vol. 2, no. 1, p. 029501, 2008. [PubMed: 23977404]

[28]. Norton SJ and Vo-Dinh T, "Plasmon resonances of nanoshells of spheroidal shape," IEEE transactions on nanotechnology, vol. 6, no. 6, pp. 627–638, 2007. [PubMed: 23976876]

[29]. Yuan H, Khoury CG, Hwang H, Wilson CM, Grant GA, and Vo-Dinh T, "Gold nanostars: surfactant-free synthesis, 3D modelling, and two-photon photoluminescence imaging," Nanotechnology, vol. 23, no. 7, p. 075102, 2012. [PubMed: 22260928]

[30]. Sordillo LA, Pu Y, Pratavieira S, Budansky Y, and Alfano RR, "Deep optical imaging of tissue using the second and third near-infrared spectral windows," J. Biomed. Opt, vol. 19, no. 5, p. 056004, 5 2014, doi: 10.1117/1.JBO.19.5.056004. [PubMed: 24805808]

[31]. Odion RA, Strobbia P, Crawford BM, and Vo-Dinh T, "Inverse surface-enhanced spatially offset Raman spectroscopy (SESORS) through a monkey skull," Journal of Raman Spectroscopy, vol. 49, no. 9, pp. 1452–1460, 9. 2018, doi: 10.1002/jrs.5402.

[32]. Yuan H, Fales AM, and Vo-Dinh T, "TAT peptide-functionalized gold nanostars: enhanced intracellular delivery and efficient NIR photothermal therapy using ultralow irradiance," Journal of the American Chemical Society, vol. 134, no. 28, pp. 11358–11361, 2012. [PubMed: 22734608]

[33]. Kereselidze Z, Romero VH, Peralta XG, and Santamaria F, "Gold Nanostar Synthesis with a Silver Seed Mediated Growth Method," JoVE, no. 59, p. 3570, 1. 2012, doi: 10.3791/3570.

[34]. Senthil Kumar P, Pastoriza-Santos I, Rodríguez-González B, Javier García de Abajo F, and Liz-Marzán LM, "High-yield synthesis and optical response of gold nanostars," Nanotechnology, vol. 19, no. 1, p. 015606, 1. 2008, doi: 10.1088/0957-4484/19/01/015606. [PubMed: 21730541]

[35]. Norton SJ and Vo-Dinh T, "Photothermal effects of plasmonic metal nanoparticles in a fluid," Journal of Applied Physics, vol. 119, no. 8, p. 083105, 2. 2016, doi: 10.1063/1.4942623.

[36]. Dhawan A, Gerhold M, and Vo-Dinh T, "Theoretical Simulation and Focused Ion Beam Fabrication of Gold Nanostructures for Surface-Enhanced Raman Scattering (SERS)," Nanobiotechnol, vol. 3, no. 3, pp. 164–171, 12. 2007, doi: 10.1007/s12030-008-9017-x.

[37]. Khoury CG, Norton SJ, and Vo-Dinh T, "Plasmonics of 3-D nanoshell dimers using multipole expansion and finite element method," Acs Nano, vol. 3, no. 9, pp. 2776–2788, 2009. [PubMed: 19678677]

[38]. Yuan H et al., "Plasmonics-enhanced and optically modulated delivery of gold nanostars into brain tumor," Nanoscale, vol. 6, no. 8, pp. 4078–4082, 2014, doi: 10.1039/C3NR06770J. [PubMed: 24619405]

[39]. Liu Y et al., "Non-invasive sensitive brain tumor detection using dualmodality bioimaging nanoprobe," Nanotechnology, vol. 30, no. 27, p. 275101, 4. 2019, doi: 10.1088/1361-6528/ab0e9c. [PubMed: 30856613]

[40]. Bernardi RJ, Lowery AR, Thompson PA, Blaney SM, and West JL, "Immunonanoshells for targeted photothermal ablation in medulloblastoma and glioma: an in vitro evaluation using human cell lines," J Neurooncol, vol. 86, no. 2, pp. 165–172, 1. 2008, doi: 10.1007/s11060-007-9467-3. [PubMed: 17805488]

[41]. Chowdhury F, Dunn S, Mitchell S, Mellows T, Ashton-Key M, and Gray JC, "PD-L1 and CD8+PD1+ lymphocytes exist as targets in the pediatric tumor microenvironment for immunomodulatory therapy," OncoImmunology, vol. 4, no. 10, p. e1029701, 10. 2015, doi: 10.1080/2162402X.2015.1029701.

[42]. Inman BA, Frigola X, Dong H, and Kwon ED, "Costimulation, Coinhibition and Cancer," Current Cancer Drug Targets, vol. 7, no. 1, pp. 15–30, 2. 2007, doi: 10.2174/156800907780006878. [PubMed: 17305475]

[43]. Bellmunt J et al., "Association of PD-L1 expression on tumor-infiltrating mononuclear cells and overall survival in patients with urothelial carcinoma," Annals of Oncology, vol. 26, no. 4, pp. 812–817, 4. 2015, doi: 10.1093/annonc/mdv009. [PubMed: 25600565]

[44]. Inman BA, Longo TA, Ramalingam S, and Harrison MR, "Atezolizumab: A PD-L1–Blocking Antibody for Bladder Cancer," Clin Cancer Res, vol. 23, no. 8, pp. 1886–1890, 4. 2017, doi: 10.1158/1078-0432.CCR-16-1417. [PubMed: 27903674]

[45]. Garg AD, Nowis D, Golab J, Vandenabeele P, Krysko DV, and Agostinis P, "Immunogenic cell death, DAMPs and anticancer therapeutics: An emerging amalgamation," Biochimica et Biophysica Acta (BBA) - Reviews on Cancer, vol. 1805, no. 1, pp. 53–71, 1. 2010, doi: 10.1016/j.bbcan.2009.08.003. [PubMed: 19720113]

[46]. Vo-Dinh T and Inman BA, "What potential does plasmonics-amplified synergistic immuno photothermal nanotherapy have for treatment of cancer?," Nanomedicine, vol. 13, no. 2, pp. 139–144, 12. 2017, doi: 10.2217/nnm-2017-0356.

[47]. Vo-Dinh T, Biomedical photonics handbook: biomedical diagnostics. CRC press, 2014.

[48]. Frens G, “Controlled Nucleation for the Regulation of the Particle Size in Monodisperse Gold Suspensions,” Nature Physical Science, vol. 241, no. 105, Art. no. 105, 1. 1973, doi: 10.1038/physci241020a0.

[49]. Hirsch LR et al., “Metal Nanoshells,” Ann Biomed Eng, vol. 34, no. 1, pp. 15–22, 3. 2006, doi: 10.1007/s10439-005-9001-8. [PubMed: 16528617]

[50]. Jain PK and El-Sayed MA, “Universal Scaling of Plasmon Coupling in Metal Nanostructures: Extension from Particle Pairs to Nanoshells,” Nano Lett., vol. 7, no. 9, pp. 2854–2858, 9. 2007, doi: 10.1021/nl071496m. [PubMed: 17676810]

[51]. Gobin AM, Moon JJ, and West JL, “EphrinAl-targeted nanoshells for photothermal ablation of prostate cancer cells,” Int J Nanomedicine, vol. 3, no. 3, pp. 351–358, 9. 2008. [PubMed: 18990944]

[52]. Liu S-Y, Liang Z-S, Gao F, Luo S-F, and Lu G-Q, “In vitro photothermal study of gold nanoshells functionalized with small targeting peptides to liver cancer cells,” J Mater Sci: Mater Med, vol. 21, no. 2, pp. 665–674, 2. 2010, doi: 10.1007/s10856-009-3895-x. [PubMed: 19834788]

[53]. Schwartz JA et al., “Feasibility Study of Particle-Assisted Laser Ablation of Brain Tumors in Orthotopic Canine Model,” Cancer Res, vol. 69, no. 4, pp. 1659–1667, 2. 2009, doi: 10.1158/0008-5472.CAN-08-2535. [PubMed: 19208847]

[54]. Pitsillides CM, Joe EK, Wei X, Anderson RR, and Lin CP, “Selective Cell Targeting with Light-Absorbing Microparticles and Nanoparticles,” Biophysical Journal, vol. 84, no. 6, pp. 4023–4032, 6. 2003, doi: 10.1016/S0006-3495(03)75128-5. [PubMed: 12770906]

[55]. Zharov VP, Galitovsky V, and Viegas M, “Photothermal detection of local thermal effects during selective nanophotothermolysis,” Appl. Phys. Lett, vol. 83, no. 24, pp. 4897–4899, 12. 2003, doi: 10.1063/1.1632546.

[56]. Abadeer NS and Murphy CJ, “Recent Progress in Cancer Thermal Therapy Using Gold Nanoparticles,” J. Phys. Chem. C, vol. 120, no. 9, pp. 4691–4716, 3. 2016, doi: 10.1021/acs.jpcc.5b11232.

[57]. Kou L, Labrie D, and Chylek P, “Refractive indices of water and ice in the 0.65- to 2.5-μm spectral range,” Appl. Opt., AO, vol. 32, no. 19, pp. 3531–3540, 7. 1993, doi: 10.1364/AO.32.003531.

[58]. Minkowycz W, Advances In Numerical Heat Transfer. CRC Press, 1996.

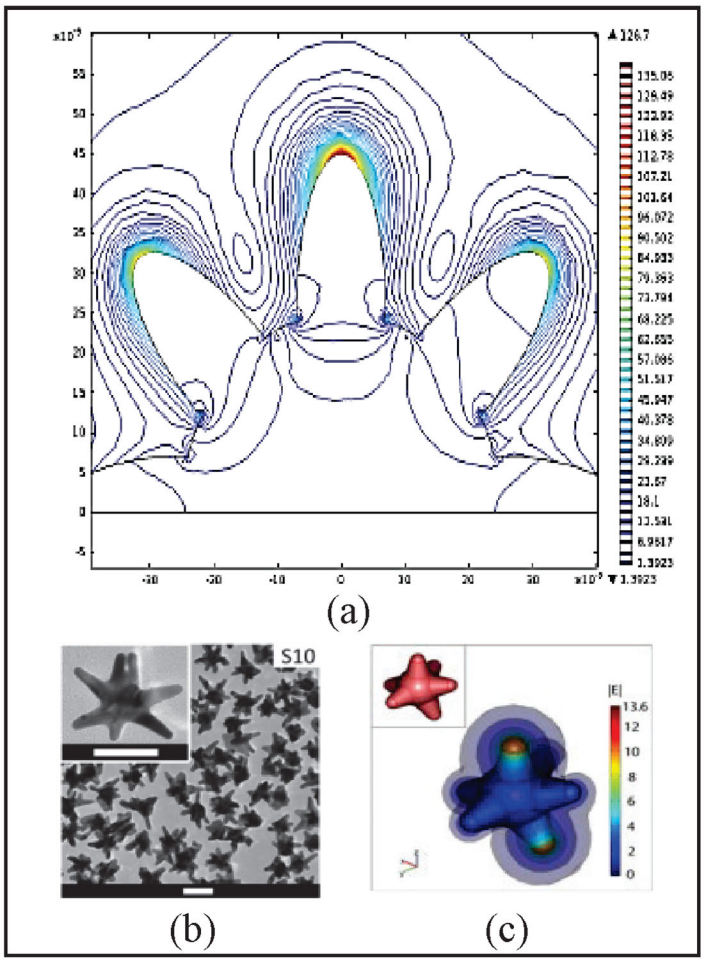

Fig. 1:

(a) Contour plot of the magnitude of the electric field showing the largest E-field enhancement occurring at the tips of the branches of the star (Adapted from Ref. 3). Scale bar is 50 nm. (b) Transmission electron microscopy image of GNS. (c) Whole 3D model and simulation of electromagnetic field around a GNS (Adapted from Ref. 29)

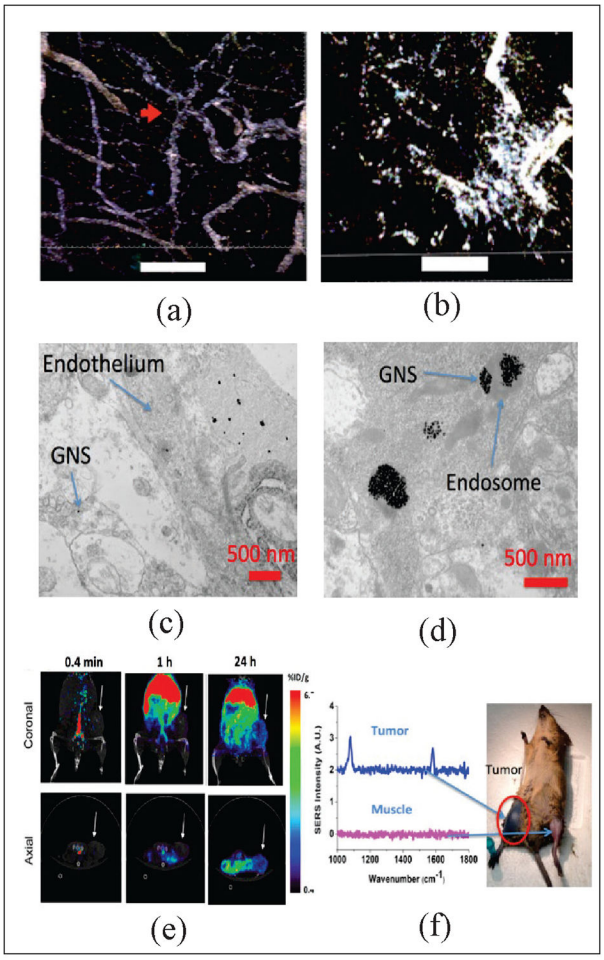

Fig. 2:

(a-b) Two-photon photoluminescence image of blood-brain barrier interface of glioblastoma model on mice treated with GNS and PTT (scale bar: 100 μm). GNS (white) initially only inside blood vessels, but after some time they are found extravasating into the surrounding parenchyma (Adapted from Ref. 38). (a) Image just before treatment. The red arrow denotes vascular tortuosity. (b) Image 48 hours after laser treatment. (c) Electron microscopy also shows that GNS nanoparticles penetrate through brain tumor vasculature and (d) can get inside the brain cancer cell (Adapted from Ref. 39). (e) PET/CT of GNS ^{64}Cu 0.4 min, 1h and 24h after IV injection. The GNS accumulate in tumor over time (Adapted from Ref. 6) (f) SERS spectra of PMBA labeled GNS in tumor flank compared to SERS at nearby muscle tissue (Adapted from Ref. 16)

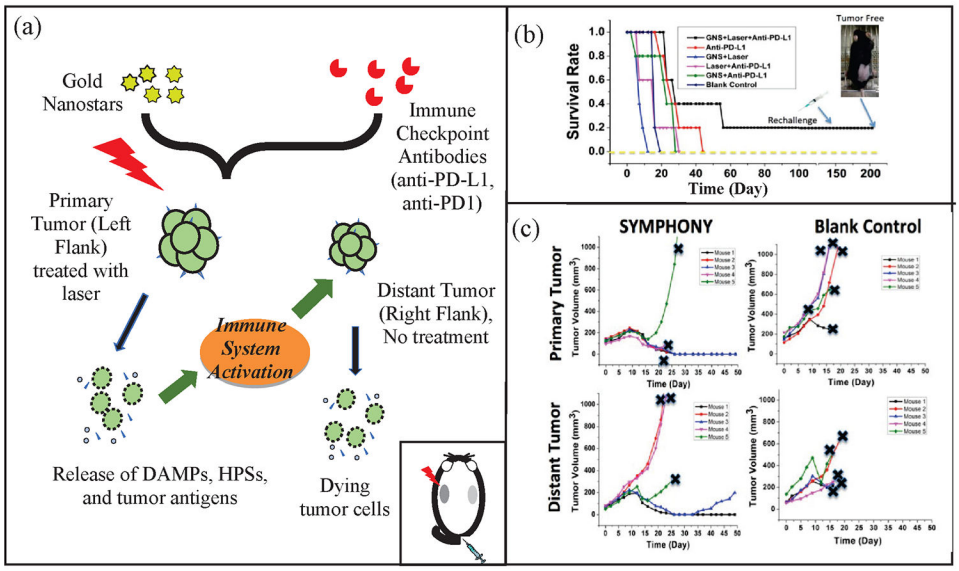

Fig. 3:

(a) SYMPHONY treatment with dual flank bladder cancer tumor (Adapted from Ref. 18) Colored orange are tumor cells. After PTT at the primary tumor, tumor cells with GNS are selectively destroyed and subsequently invokes an immune response. Afterwards, the immune response can target the distant right flank tumor. (b) Kaplan-Meier survival curve of mice in SYMPHONY study. The tumor-free mouse in SYMPHONY group was monitored for 3 months and no tumor recurred. A rechallenge was performed after 150 days and no tumor developed (Adapted from Ref. 18) (c) Tumor size for both the primary and distant tumor was also monitored. Note that only the primary tumor received laser treatment, thus indicating the SYMPHONY treatment's effectiveness in reducing distant tumor sizes despite not having direct thermal treatment (Adapted from Ref. 18).

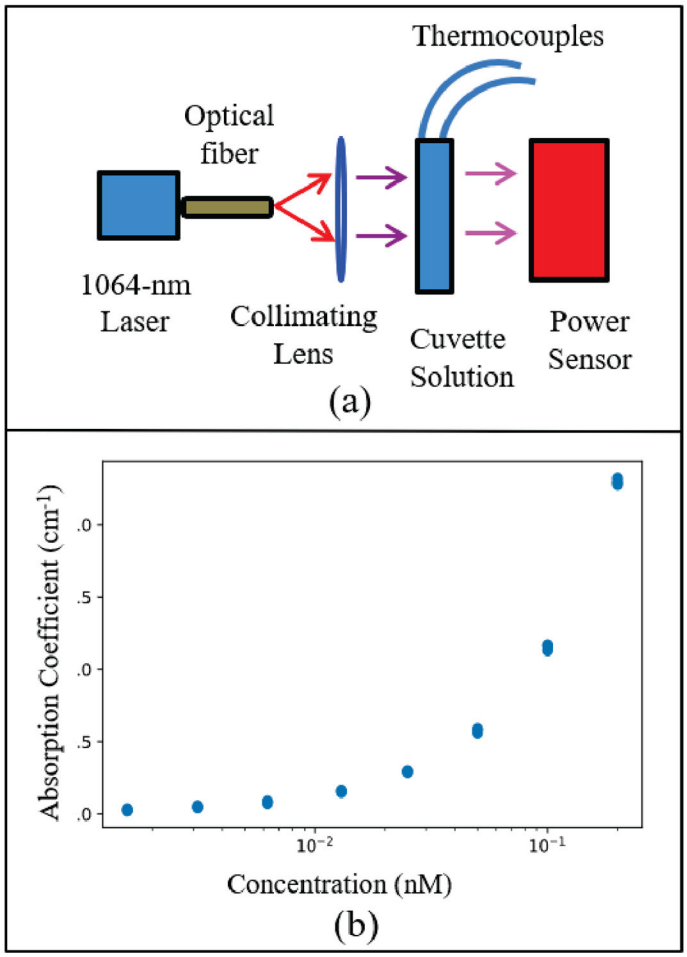

Fig. 4:

(a) Optical transmission configuration for determining optical and photothermal properties of GNS at 1064-nm excitation. (b) Log-scale plot of absorption coefficient of GNS as a function of concentration in nanomolar.

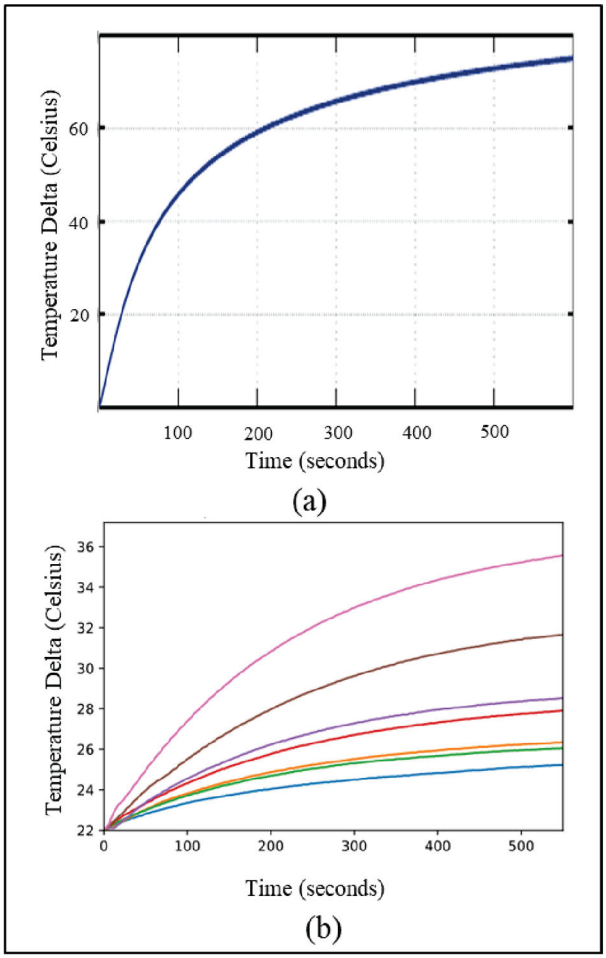

Fig. 5:

(a) Theoretically derived time evolution of heating of a GNS solution under excitation of the plasmon resonance (Adapted from Ref. 35). (b) Experimentally collected heating data over time showing a similar heating profile as the theoretical model.

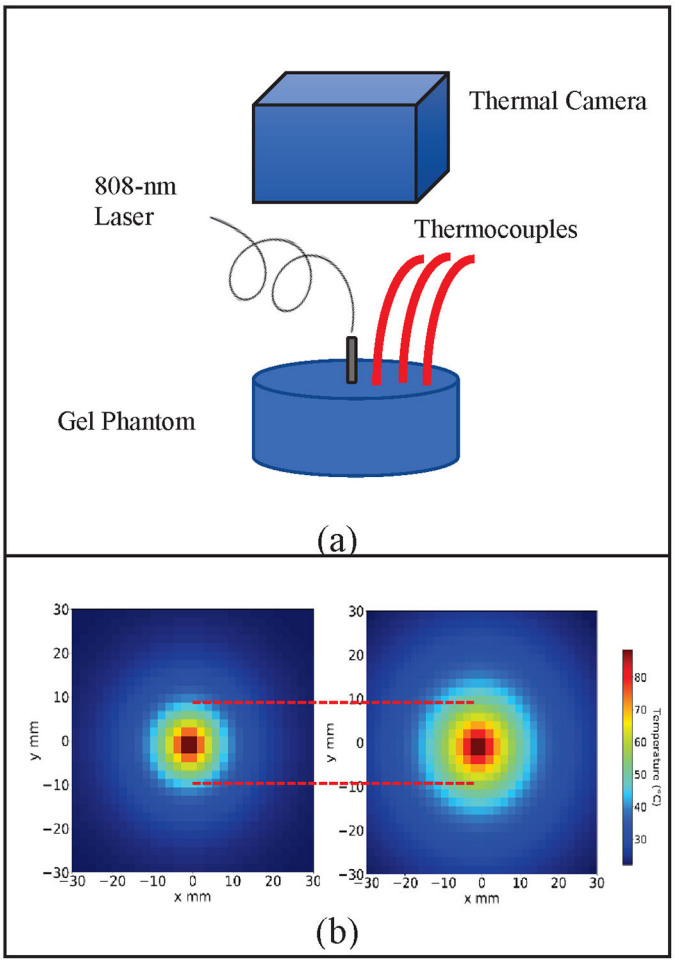

Fig. 6:

(a) Spatial heating data collection configuration with thermocouples placed at 10 mm, 13 mm, and 15 mm away from the center heating probe of gel phantom containing GNS. (b) Spatial map extrapolation of heating of GNS-embedded gel phantom measured after 400 seconds. The left plot shows the heating of the gel with no GNS while the right plot shows the heating of the gel having GNS. The increase in spatial heating of the GNS-containing gel is clearly shown after the same time point.